Temperature dependence of phonon-assisted excitation probability in $GdTb(MoO_4)_3$: Evidence for a change in electron-lattice coupling near a structural phase transition

P. Raveendran
Department of Chemistry and Regional Sophisticated Instrumentation Centre, Indian Institute of Technology, Madras 600 036, India

N. Sukumar
Theorie International, 175 Lloyds Road, Gopalapuram, Madras 600 036, India

T. K. K. Srinivasan*
Department of Chemistry and Regional Sophisticated Instrumentation Centre, Indian Institute of Technology, Madras 600 036, India
(Received 11 July 1996; revised manuscript received 4 October 1996)

Temperature dependence of the intensity of the phonon-assisted excitation probability (as a function of the intensity of the luminescence bands corresponding to the $^5D_4 \rightarrow {}^7F_J$ transitions) of Tb^{3+} ion in $GdTb(MoO_4)_3$ (GTMO), above and below the ferroelectric phase transition temperature (T_c) is investigated in the present work. The experiments reveal a sharp change in the intensity near T_c. This change is attributed to a sharp change in the electron-phonon coupling near T_c. A phenomenological model is proposed to fit the experimental data, in broad accordance with the Ginzburg-Landau equations for critical behavior. The investigations also clearly indicate that phonon-assisted excitation probability can be used to probe structural phase transitions. [S0163-1829(97)05108-4]

I. INTRODUCTION

Phonon-assisted electronic excitation is associated with a shift in the equilibrium position of the lattice coordinates[1,2] and a positive value for the Pekar-Huang-Rhys (PHR) coupling constants.[2] The intensity of phonon-assisted luminescence is proportional to the probability of the phonon-assisted excitation, which in turn depends not only on the population of the phonon states, but also on the strength of the electron-phonon coupling present in the given solid-state matrix (the luminescence intensity also depends upon other factors such as the nonradiative decay and the interion energy transfer).[2,3] Thus phonon-assisted luminescence intensity can be used as a probe to investigate the difference in electron-phonon coupling behavior in different solid-state matrices. Auzel reported the phonon-assisted luminescence spectra of rare-earth (Er^{3+} and Ho^{3+}) ions doped in LaX_3 matrices (X denotes the halogen atom).[4,5] Rare-earth ions are distinct for their characteristic weak electron-phonon coupling.[6] Also, a change in electron-lattice coupling during a structural phase transition can be reflected in the intensity of the phonon-assisted luminescence bands. The nonradiative decay and interion energy transfer also depend on the strength of electron-lattice coupling[2] in the lattice. However, Auzel[7] has indicated that the same S value may not hold good for both the phonon-assisted excitation and the nonradiative decay as he has established that different phonons could be responsible for these processes. Thus the temperature dependence of the phonon-assisted luminescence intensity in the vicinity of a structural phase transition is extremely interesting. However, to the best of our knowledge, no such work has been reported to date.

In the present work, we investigate the temperature dependence of the intensity of the phonon-assisted anti-Stokes luminescence bands corresponding to the $^5D_4 \rightarrow {}^7F_J$ transitions of the Tb^{3+} ion in $GdTb(MoO_4)_3$ (GTMO) matrix, which undergoes a ferroelectric-paraelectric structural phase transition at around 433 K.[8] In the low-temperature phase, far from phase transition, the temperature dependence of the intensity is in accordance with the behavior expected of the simple Miyakawa-Dexter theory.[2,3] However, close to phase transition, the theory with a single, invariant electron-phonon coupling parameter no longer suffices to explain the observed behavior, and the effects of structural phase transition also need to be explicitly included.

II. THEORY

The ground-state electronic configuration of the Tb^{3+} ion has eight $4f$ electrons outside the closed orbitals. In this configuration, the ground LS term is the rather isolated ^7F, which further splits into seven nondegenerate levels due to spin-orbit coupling. The lowest level of the next term $^5D_4$ acts as the upper fluorescence level in the Tb^{3+} ion. The selection rules for the transitions have been developed by Judd[9(a)] and Ofelt.[9(b)] For the electric dipole (ED) transitions, assuming a static model and pure electronic transitions, the selection rules are $\Delta S=0$, $\Delta L \leqslant 6$, and $\Delta J \leqslant 6$. However, intermediate coupling removes L and S as good quantum numbers. In most cases J mixing is negligibly small. The selection rules for magnetic dipole transitions are $\Delta J=0, \pm 1$ where $0 \leftrightarrow 0$ transitions are forbidden. In structures where the Tb^{3+} ion occupies a low symmetry site, as in the case of GTMO where it occupies a C_1 site, transitions between the $^5D_4$ and all levels of the ^7F_J multiplet are possible. The excitation maximum for the $^7F_6 \rightarrow {}^5D_4$ transition is at 487 nm ($\approx$20534 cm^{-1}).

The term ''anti-Stokes excitation'' generally refers to the excitation of electrons from a state of higher energy than the ground electronic state of the ion. In phonon-assisted anti-

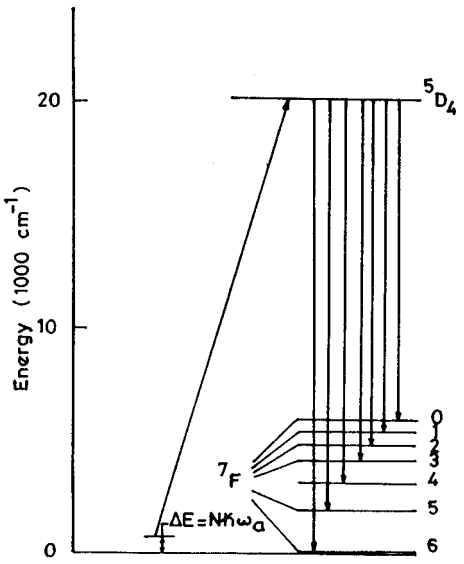

FIG. 1. A schematic representation of the phonon-assisted anti-Stokes excitation and the luminescence emissions of Tb^{3+} ion. Here ΔE is the energy gap spanned by electron-phonon coupling (N is the order of the multiphonon process and ω_a is the frequency of the phonon coupling with the electrons).

Stokes excitation, the energy of the exciting radiation is less than the energy gap between the ground and the excited electronic states and the additional energy (ΔE) is supplemented at the cost of the vibrational energy of the system, through electron-phonon coupling. A schematic representation of such an anti-Stokes excitation and the corresponding emissions of Tb^{3+} ion is shown in Fig. 1. Here $\Delta E = N\hbar\omega_a$, N being the order of the multi-phonon process and ω_a, the frequency of the phonon coupling with the electron. Throughout this paper, we use the term ''phonon-assisted luminescence'' to describe the emission resulting from phonon-assisted anti-Stokes excitation, to differentiate it from the one corresponding to the normal electronic excitation from the electronic ground state.

Miyakawa and Dexter[2] outlined a common theoretical treatment for all three phonon-assisted processes, viz., phonon-assisted electronic excitation, nonradiative decay, and interion energy transfer. Using the adiabatic or Born-Oppenheimer (BO) approximation[10–12] in dealing with the lattice vibrations, one solves for the eigenvalues and eigenfunctions of electrons for fixed lattice coordinates Q (where r and Q denote the coordinates of electrons and the lattice, respectively). The Q-dependent electronic energy eigenvalue $E_j(Q)$ is then used as the state-dependent effective potential for the lattice vibrations. The total wave function $\Psi_{jv}(r,Q)$ is then written as a product of the electronic wave function $\Phi_j(r,Q)$ and the lattice wave function $X_{jv}(Q)$. These are not strictly stationary states of the system, because of the Q dependence of the electronic wave functions $\Phi_j(r,Q)$. The terms left out of the BO approximation constitute the Born coupling terms,[11,13,14] which cause nonradiative transitions between the electronic levels. Similarly, ion-ion interactions also cause energy transfer between states of the system.[2,15]

The adiabatic approximation is applicable[2,11,12] for systems where coupling through electron-radiation, interion, and nonadiabatic interaction terms are weak compared with that through the electron-lattice interaction, so that the wave functions $\Psi_{jv}(r,Q)$ serve as good zero-order functions. A general linear interaction $-\Sigma_s V_s(r)Q_s$ is assumed (the sum being over all lattice modes **s**) and the wave functions $\Phi_j(r,Q)$ and adiabatic potentials $U_j(Q)$ are expanded pertubatively. The lattice potential in the ground electronic state is diagonalized by the use of the lattice normal modes Q_s.

Using the Kubo-Toyozawa-Lax generating function method,[15] the following expression was derived[2] for the optical absorption constant $A(\nu)$ in a crystal containing N ions:

$$A(\nu)=\frac{8\pi^3 N\nu F_M(h\nu)}{3\mu c}, \tag{1}$$

where c is the velocity of light, μ is the refractive index of the crystal, and

$$F_M(E)=\sum_{v,v'}|\langle f|\mathbf{M}|i\rangle|^2 W_i\delta(E-E_f+E_i) \tag{2}$$

is the spectral function for the interaction M; f and i label the final (kv') and initial (jv) states. W_i is the Boltzmann distribution for the initial phonon states in thermal equilibrium with the surroundings at temperature T. The operator M for the case of optical absorption, is the dipole moment operator. The spectral function $F_M(E)$ is expressed in terms of the generating function $f_M(t)$, defined as the Laplace transform of $F_M(E)$:

$$f_M(t)=\int_{-\infty}^{\infty}F_M(E)e^{-tE}dE=\exp\left\{\frac{-i\Delta\epsilon t}{\hbar}-\int d\omega D(\omega)\right.$$
$$\left.\times[2n_\omega(\cos\omega t-1)+\exp(-i\omega t)-1]\right\}, \tag{3}$$

$\Delta\epsilon$ being the energy gap between the two levels.

$$D(\omega)=\sum_s\frac{\omega_s\Delta_s^2\delta(\omega-\omega_s)}{2\hbar} \tag{4}$$

is the spectral density of the electron-phonon coupling which specifies the strength and spectral distribution of electron-phonon coupling in the given solid state matrix.

$$\Delta_s=Q_s(k)-Q_s(j) \tag{5}$$

is the shift in the equilibrium position of the lattice normal coordinates, and

$$n_\omega(T)=\frac{1}{e^{\beta\hbar\omega}-1}. \tag{6}$$

An ion in a crystal undergoing phonon-assisted excitation at the laser frequency ν' can decay radiatively by the emission of a photon, can decay nonradiatively as a result of the nonadiabatic coupling terms, or can transfer the excitation to an adjacent ground state ion through interion interaction. The nonradiative decay and interion energy transfer mechanisms are common to both the normal and phonon-assisted processes. To explain the experimental temperature-dependence of the phonon-assisted luminescence, Auzel,[3,4] using the modified ''Pekarian'' form, derived the following expression

for the probability of phonon-assisted anti-Stokes excitation:

$$W_{\mathrm{AS}}=\frac{8\pi^3 I(\nu)}{3h^2c}\,|\mathbf{M}|^2\,\frac{e^{-s}s^N}{N!}\,n_\omega^N. \tag{7}$$

Here $N=\Delta E/\hbar\omega_a$ is the order of the multiphonon excitation process, ω_a being the frequency of the phonon coupling with the electron (generally we consider the phonon with the highest energy) and $I(\nu)$ is the intensity of the incident radiation of frequency ν. In the present experiment, for the phonon-assisted excitation of the Tb^{3+} ion in GTMO using 514.5-nm excitation, the energy gap to be spanned by phonon coupling is 1098 cm^{-1} (20 534–19 436 cm^{-1}). Hence the order of the phonon process in the present case is $N\approx 1$.

III. EXPERIMENT

The ferroelectric to paraelectric, first-order phase transitions in $Gd_2(MoO_4)_3$ (GMO) and $Tb_2(MoO4)_3$ (TMO) have been extensively studied using various techniques. In both these systems, the phase transitions occur at around 433 K.[8,16–21] GTMO is isostructural with GMO and undergoes a first-order structural phase transition from $Pba2$ $(z=4)$ to $P42_1m$ $(z=2)$ at around 433 K. The low-temperature phase is an improper ferroelectric and the high-temperature phase is paraelectric. As our studies reveal, this phase transition modifies the electron-phonon coupling behavior in the lattice and produces drastic changes in the intensity pattern of the phonon-assisted luminescence bands corresponding to the $^5D_4\rightarrow{}^7F_J$ transitions of the Tb^{3+} ion in GTMO. This is the focus of our experimental investigations presented in the following sections.

Melt-grown (Czochralski method), polished, single crystals of GTMO of size 5×3×2 mm are used for investigations. The normal luminescence spectra are recorded using a Hitachi-F-4500 fluorescence spectrometer. Phonon-assisted luminescence spectra are recorded using a Dilor Z24 single channel spectrometer equipped with the 514.5-nm excitation of an argon-ion laser. The temperature at the sample is controlled to an accuracy of ±2.

IV. RESULTS AND DISCUSSION

The normal luminescence spectrum of GTMO recorded using 487-nm excitation is presented in Fig. 2(a). The doublet appearing at around 542 nm corresponds to the $^5D_4\rightarrow{}^7F_5$ emission of the Tb^{3+} ion while the weak bands around 582 and 619 nm correspond to the $^5D_4\rightarrow{}^7F_4$ and $^5D_4\rightarrow{}^7F_3$ transitions, respectively. The absorption spectrum (solid curve) and the excitation spectrum for 542-nm emission (dotted curve) of GTMO are shown in Fig. 2(b). The absorption and excitation spectra are almost identical with their maxima at around 487 nm but for a weak side band at 467 nm in the excitation spectrum.

The different regions of the Raman spectrum of GTMO recorded using the 514.5-nm (19 436 cm^{-1}) excitation line of the argon ion laser are given in Fig. 3. The bands below 970 cm^{-1} in Fig. 3(a) (743, 802, 820, 825, 848, 853, 942, and 958 cm^{-1}) correspond to the internal vibrational modes[22] of the molybdate group. The other bands correspond to the phonon-assisted luminescence bands corresponding to the $^5D_4\rightarrow{}^7F_J$ transitions. Since the spectra are recorded using a Raman spectrometer, the positions of the luminescence bands are given in terms of the Raman shift with respect to the excitation line and the actual energy corresponding to the particular electronic transition is given by the difference between the excitation energy and the corresponding Raman shift. The fine structure associated with these bands results from the crystal field effects. The strongest band at 1010 cm^{-1} (actual energy 19 436–1010=18 426 cm^{-1}) and the one at 1185 cm^{-1} (actual energy=18 251 cm^{-1}) in Fig. 3(a) correspond to the $^5D_4\rightarrow{}^7F_5$ transition of the Tb^{3+} ion. The bands at around 2332 cm^{-1} (actual energy 17 104 cm^{-1}) and 2534 cm^{-1} (actual energy 16 902 cm^{-1}) in Fig. 3(b) correspond to the $^5D_4\rightarrow{}^7F_4$ emission and the one around 3282 cm^{-1} (actual energy 16 154 cm^{-1}) in Fig. 3(c) corresponds to the $^5D_4\rightarrow{}^7F_3$ emission. The broad, weak band at around -1050 cm^{-1} (anti-Stokes region of the Raman spectrum) in Fig. 3(d) corresponds to the anti-Stokes, $^5D_4\rightarrow{}^7F_6$ emission.

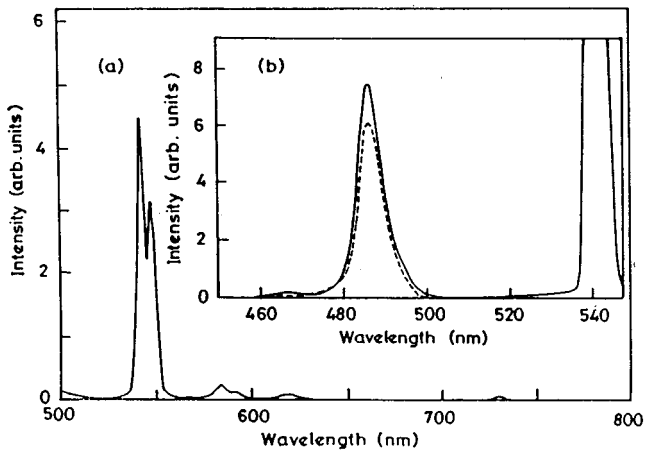

FIG. 2. (a) Normal luminescence of GTMO (487-nm excitation) corresponding to $^5D_4\rightarrow{}^7F_J$ emissions. (b) The excitation spectrum (solid curve) of GTMO for 542-nm emission and the absorption spectrum (dotted curve).

The 800–1300-cm^{-1} region of the Raman spectra at different temperatures below and above T_c (433 K) is given in Fig. 4. The bands appearing at 942 and 958 cm^{-1} correspond to the stretching vibrations of the molybdate group[22] while those at 1010 (actual energy 18 426 cm^{-1}) and 1185 cm^{-1} (actual energy 18 251 cm^{-1}) are the luminescence bands corresponding to the $^5D_4\rightarrow{}^7F_5$ transition of the Tb^{3+} ion. The temperature dependence of the intensity of phonon-assisted anti-Stokes luminescence bands is clearly seen in Fig. 4. The intensity approaches zero at 80 K. Above room temperature, the intensity increases with temperature up to T_c, but then decreases rather sharply. A plot of the intensity of the 1010-cm^{-1} band against temperature is given in Fig. 5(a). While the temperature dependence is in good accordance with Eq. (7) up to temperatures close to T_c, it is quite evident that the Miyakawa-Dexter theory[2] with an invariant S breaks down near the phase transition. Thus we write a phenomenological equation to fit the observed intensity data. Taking $N\approx 1$, Eq. (7) can be rewritten in the form

$$I_{\mathrm{AS}}=\frac{\Omega(T)}{e^{\beta\hbar\omega}-1}, \tag{8}$$

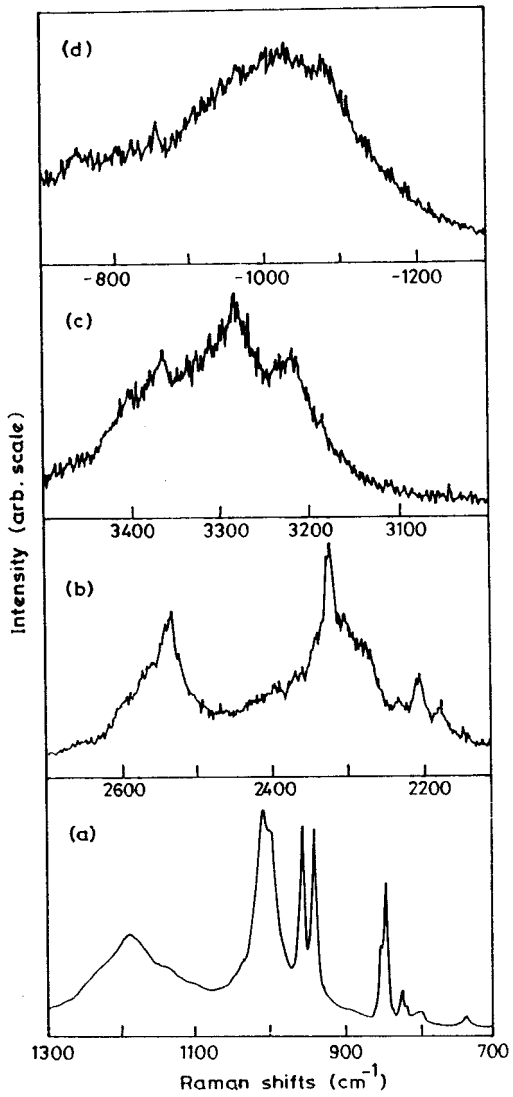

FIG. 3. Different regions of the Raman spectrum of GTMO recorded using 514.5-nm excitation. The luminescence bands at 1010 and 1185 cm^{-1} in (a) correspond to the $^5D_4 \rightarrow {}^7F_5$ emission, regions in (b), (c), and (d) correspond to the $^5D_4 \rightarrow {}^7F_4$, $^5D_4 \rightarrow {}^7F_3$, and $^5D_4 \rightarrow {}^7F_6$ emissions, respectively.

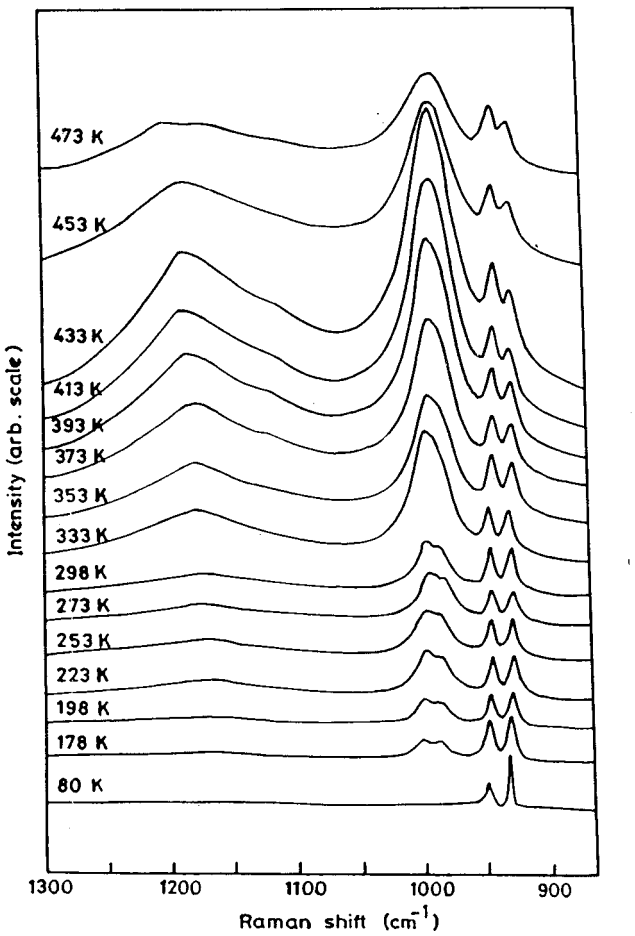

FIG. 4. The 800–1300-cm^{-1} region of the Raman spectra of GTMO at different temperatures recorded using 514.5-nm excitation. The bands at 1010 and 1185 cm^{-1} correspond to the phonon-assisted luminescence ($^5D_4 \rightarrow {}^7F_5$ emissions). The phase transition occurs at 433 K.

where we have retained the n_ω factor from Eq. (7); I_{AS} is the intensity of phonon-assisted luminescence. According to the Miyakawa-Dexter theory $\Omega(T)$ should not have any further temperature dependence. The experimentally observed intensity pattern suggests a linear dependence of the PHR coupling parameter S on the absolute value of $(T-T_c)$:

$$\Omega(T) \propto S(T) e^{-S(T)}, \tag{9}$$

$$S(T) \approx C|T-T_c| + C_0, \tag{10}$$

with different values of C for $T<T_c$ and $T>T_c$. Figure 5(a) also shows a theoretical fit to the experimental intensity data, based on Eqs. (8)–(10) with $C_{T<T_c}=1.95\times10^{-5}$ and $C_{T>T_c}=2.6\times10^{-4}$ K^{-1}.

Thus we see clear evidence for a change in the electron-phonon coupling behavior in the vicinity of T_c. The temperature dependence given by Eqs. (8)–(10) is in broad accordance with that expected from the Ginzburg-Landau theory for critical phenomena; the value of the critical exponent being unity and the value of S going to a minimum at T_c.

The temperature dependence of the normal luminescence bands corresponding to the $^5D_4 \rightarrow {}^7F_5$ emission (542 nm) is also investigated and a plot of the intensity against temperature is provided in Fig. 5(b). The temperature dependence is in good accordance with the Boltzmann factor (as the rates of nonradiative decay and interion energy transfer increase with increase in temperature, the luminescence intensity decreases with temperature) and there is no observable change in this behavior near T_c. This is surprising at first sight, as the rates of nonradiative decay and interion energy transfer also depend on the electron-phonon coupling parameter in a similar manner. However, this can be explained on the basis of the experimental observations of Auzel,[7] who pointed out that the phonons responsible for phonon-assisted excitation are often different from the ones responsible for nonradiative decay and interion energy transfer. In view of this we feel that we should consider two different S values for these pro-

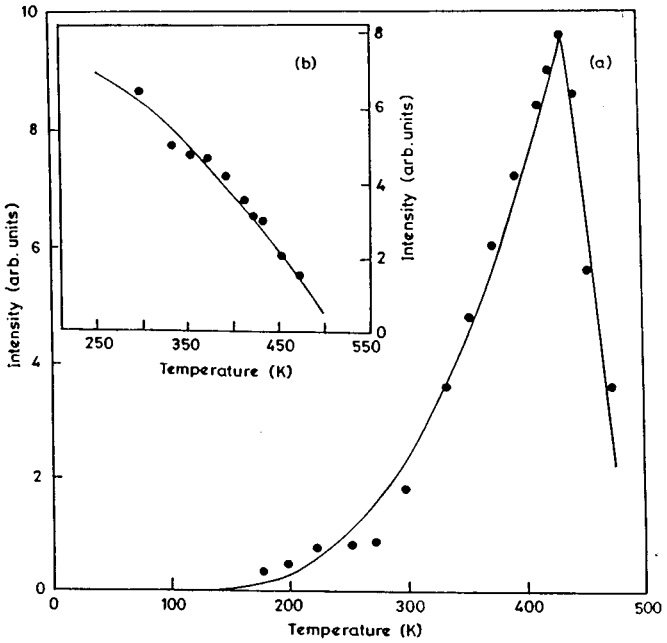

FIG. 5. (a) Plot of Intensity vs temperature for the 1010-cm^{-1} (phonon-assisted luminescence) band in the Raman spectrum of GTMO. The solid circles indicate the experimental data while the solid curve corresponds to the theoretical fit based on equations (8)–(10). (b) Plot of intensity vs temperature for the normal luminescence corresponding to the $^5D_4 \rightarrow {}^7F_5$ emission of the Tb^{3+} ion in GTMO. The phase transition occurs at 433 K.

cesses and that while the S for phonon-assisted excitation undergoes a drastic modification near T_c, there is no such change in the S for the nonradiative decay and interion energy transfer.

Pressure-induced phase transitions can also modify the intensity pattern of the phonon-assisted luminescence bands. This effect is contained in the high-pressure Raman studies of TMO reported by Kourouklis, Ves, and Christofilos[23] using the 514.5-nm excitation line, which reveal a pressure-induced phase transition occurring at around 2 GPa. The spectrum recorded at 1.4 GPa clearly shows the presence of the phonon-assisted luminescence bands at 1010 and 1185 cm^{-1} (corresponding to the $^5D_4 \rightarrow {}^7F_5$ transition) while these bands are almost absent in the spectrum at 2.7 GPa. The sudden change in the intensity of these bands can be attributed to the drastic change in the electron-phonon coupling as a result of the phase transition at 2 GPa. The authors,[23] however, describe these bands just as normal photoluminescence bands. The results clearly indicate that pressure-induced structural phase transitions also modify the electron-phonon coupling behavior in the lattice.

The exact mechanism of the microscopic process conducing to the observed behavior is yet to be investigated. However, it seems quite possible that the coupling between the electrons and the molybdate stretching modes (which presumably couple with the electrons) goes down as a result of the reorientation of the molybdate tetrahedra, during the phase transition.[8]

ACKNOWLEDGMENTS

We sincerely thank Dr. Sheik Saleem for providing the GTMO crystal and Professor S. Subramanian and Dr. Babu Varghese for fruitful discussions. The financial support of CSIR to PR is gratefully acknowledged.

*Electronic address: ssg!lisa@iitm.ernet.in

[1] T. Miyakawa, in *Luminescences of Crystals, Molecules and Solutions*, edited by F. Williams (Plenum, New York, 1973), p. 394.
[2] T. Miyakawa and D. L. Dexter, Phys. Rev. B **1**, 2961 (1970).
[3] F. Auzel, in *Luminescence of Inorganic Solids*, edited by B. Dibartolo (Plenum, New York, 1978), p. 67.
[4] F. Auzel, Phys. Rev. B **13**, 2809 (1976); F. Auzel, J. Lumin. **12–13**, 715 (1976).
[5] F. Auzel, J. Lumin. **21**, 187 (1980).
[6] W. E. Bron and W. Wagner, Phys. Rev. **139**, A233 (1965).
[7] F. Auzel and Y. H. Chen, J. Lumin. **60–61**, 101 (1994).
[8] E. T. Keve, S. C. Abrahams, and J. L. Bernstein, J. Chem. Phys. **45**, 3185 (1971); W. Jeitschko, Acta Crystallogr. **28B**, 60 (1972).
[9] (a) B. R. Judd, Phys. Rev. **127**, 750 (1962); (b) G. S. Ofelt, J. Chem. Phys. **37**, 511 (1962).
[10] M. Born and J. R. Oppenheimer, Ann. Phys. (Leipzig) **84**, 457 (1927).
[11] M. Born and K. Huang, *Dynamical Theory of Crystal Lattices* (Clarendon, Oxford, 1954), Sec. 14 and Appendices 7, 8.
[12] W. Kolos, Adv. Quantum Chem. **5**, 99 (1970).
[13] M. Born, Nachr. Akad. Wiss. Göttingen, Math-Phys. Kl. **1** (1951).
[14] Y. Zhang, N. Sukumar, J. L. Whitten, and R. N. Porter, J. Chem. Phys. **91**, 7057 (1989); N. Sukumar, Int. J. Quantum Chem. **56**, 423 (1995); Th. Neuheuser, N. Sukumar, and S. D. Peyerimhoff, Chem. Phys. **194**, 45 (1995).
[15] R. Kubo, Phys. Rev. **86**, 929 (1952); R. Kubo and Y. Toyozawa, Prog. Theor. Phys. **13**, 162 (1955); M. Lax, J. Chem. Phys. **20**, 1752 (1952).
[16] L. E. Cross, A. Fouskova, and S. E. Cummins, Phys. Rev. Lett. **21**, 812 (1968).
[17] L. H. Brixner, Rev. Chim. Minera. **10**, 47 (1973).
[18] F. G. Ullman *et al.*, Phys. Rev. B **8**, 2991 (1973).
[19] P. A. Fleury, Solid State Commun. **8**, 601 (1970).
[20] B. Dorner, J. D. Axe, and G. Shirane, Phys. Rev. B **6**, 1950 (1972).
[21] L. L. Boyer and J. R. Hardy, Phys. Rev. B **8**, 2205 (1973).
[22] S. Sheik Saleem, G. Aruldhas, and H. D. Bist, Spectrochim. Acta **39 A**, 1049 (1984); S. Sheik Saleem and T. K. K. Srinivasan, Spectrochim. Acta **41 A**, 1419 (1985).
[23] G. A. Kourouklis, S. Ves, and D. Christofilos, High Pressure Research **13**, 127 (1994).